

THE STRUCTURES OF THE MINERALS OF THE DESCLOIZITE AND ADELITE GROUPS: V—DESCLOIZITE AND CONICALCITE (PART 3). THE STRUCTURE OF DESCLOIZITE

M. M. QURASHI¹ AND W. H. BARNES

*Division of Pure Physics, National Research Council,
Ottawa, Canada*

ABSTRACT

The structure of descloizite, $\text{Pb}(\text{Zn,Cu})(\text{VO}_4)(\text{OH})$, has been refined first in $Pnma$ by two-dimensional partial-difference syntheses, followed by antisymmetrical Patterson and Fourier syntheses utilizing a very small number of observed reflections forbidden in $Pnma$, and finally in $P2_12_12_1$ by difference syntheses in which all observed reflections have been included. The structure consists of a three-dimensional assemblage of distorted VO_4 tetrahedra, $\text{ZnO}_4(\text{OH})_2$ tetragonal bipyramids, and $\text{PbO}_7(\text{OH})$ square antiprisms, sharing corners and edges. The relationship of the descloizite structure to those of conicalcrite and pyrobelonite is discussed.

INTRODUCTION

Descloizite, $\text{Pb}(\text{Zn,Cu})(\text{VO}_4)(\text{OH})$, is orthorhombic with $a = 7.607$, $b = 6.074$, $c = 9.446$ Å, $Z = 4$ (Barnes & Qurashi, 1952), and a preliminary structure, based on space group $Pnma$, has been proposed for it (Qurashi & Barnes, 1954). In this earlier investigation the positions of the lead atoms were fixed uniquely on the basis of the Patterson maps for the three principal zones, while those of the zinc and vanadium atoms were limited to two out of three possible locations. This ambiguity was removed by the first set of Fourier syntheses which also provided good indications of the sites of the oxygen atoms. The trial structure has now been refined in $Pnma$ followed by further refinement in $P2_12_12_1$. The change of space group became necessary because of the presence of four very weak $0kl$ reflections for which $k + l = 2n + 1$ (Qurashi, Barnes & Berry, 1953). The shifts of some of the atoms from $Pnma$ positions were first established with the aid of antisymmetrical Patterson and Fourier maps (Qurashi, 1963) which have recently been applied successfully in the case of the related mineral, conicalcrite $\text{CaCu}(\text{AsO}_4)(\text{OH})$, (Qurashi & Barnes, 1963).

¹Visiting Scientist from the Central Laboratories of the Pakistan Council of Scientific and Industrial Research, Karachi, Pakistan.

REFINEMENT IN *Pnma*

Refinement was started with two successive Fourier syntheses for each zone, for which the signs were obtained by ignoring the one unresolved oxygen atom in each projection. It should be noted that this oxygen atom is not the same in all three projections. The only sign left in serious doubt was that of 004, the amplitude of which is small; this reflection, therefore, was omitted temporarily. Scattering factors, originally taken from the Internationale Tabellen (1935), Viervoll & Ögrim (1949), and Qurashi (1953), were now selected from the data of Freeman (1959), interpolating, where necessary, over small ranges of Z . Initially, an isotropic temperature factor with $B = 1.5 \text{ \AA}^2$ was adopted for all atoms.

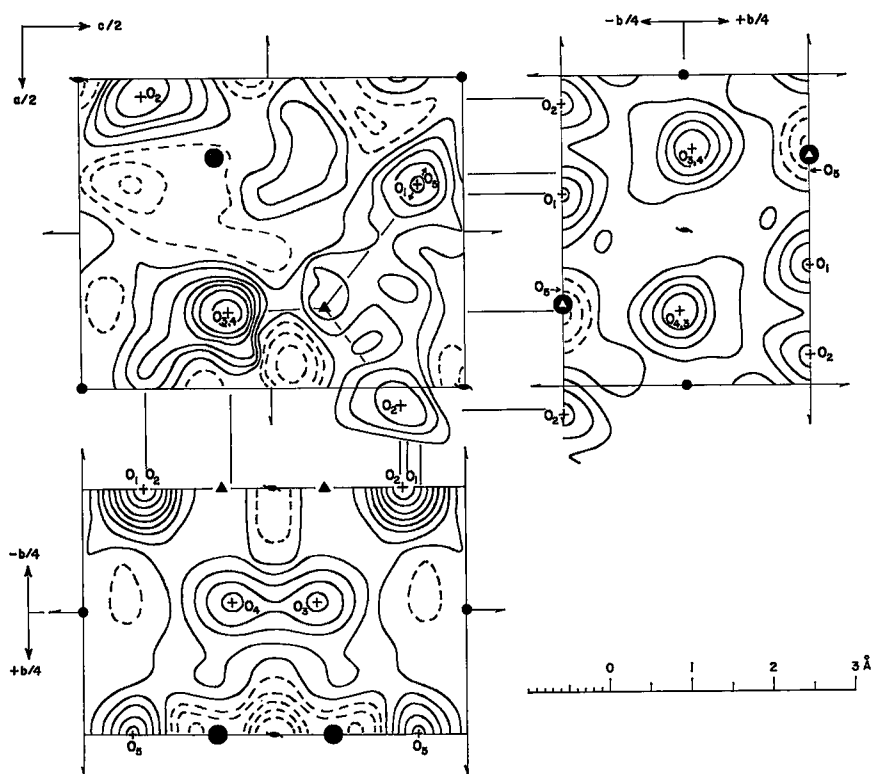


FIG. 1. Partial difference maps after preliminary refinement in *Pnma*. Large solid circles, Pb; small solid circles, Zn; triangles, V; crosses, O. Contours at intervals of $2 e \cdot \text{\AA}^{-2}$; zero and negative contours indicated by broken lines.

The co-ordinates obtained from the Fourier maps were employed in the calculation of structure factors for an $(F_o - F_{c(m)})$ -synthesis, where

$F_{c(m)}$ represents the sum of the calculated structure factors for the metal atoms (Pb, Zn, V). This partial difference synthesis was evaluated for each of the three principal zones using an additional converging factor of $\exp[-3(\sin^2\theta/\lambda^2)]$, as for the earlier Fourier syntheses. The three partial difference maps are shown in Fig. 1 where the oxygen atoms are numbered in conformity with those in pyrobelonite (Donaldson & Barnes, 1955) and in conichalcite (Qurashi & Barnes, 1963), and the broken lines drawn from one map to the next connect peaks corresponding to the same oxygen atom.

From Fig. 1 the height of a single oxygen peak is about $8.0 \pm 2 e.\text{\AA}^{-2}$, the standard deviation being based on the estimated accuracy (8–10%) of the values of $|F_o|$. On this basis, the peak labelled O_4 , of height $10.2 e.\text{\AA}^{-2}$, at $(-, -0.017, 0.197)$ and its companion, O_3 , at $(-, -0.017, 0.303)$, in the $0kl$ map, represent a pair of oxygen atoms in the 8-fold general position of $Pnma$, in agreement with the double peak ($14.9 e.\text{\AA}^{-2}$) at $(0.380, -, 0.194)$ in the $h0l$ map, and the two peaks (O_3, O_4) in the $hk0$ map. Because all the other oxygen atoms are in 4-fold positions with $y = \pm \frac{1}{4}$, some of them overlap in the maps. Thus, O_2 at $(0.538, \frac{3}{4}, 0.416)$ is clearly resolved in the $hk0$ and $h0l$ maps, with a peak height of $8.8 e.\text{\AA}^{-2}$, but it overlaps O_1 almost completely in the $0kl$ map giving a combined peak height of $17 e.\text{\AA}^{-2}$; O_1 is resolved in the $hk0$ map but partially overlaps O_5 in the $h0l$ map to produce an elongated peak ($10.2 e.\text{\AA}^{-2}$) at $(0.174, -, 0.442)$. The atom O_5 at $0.139, \frac{1}{4}, 0.417$ is clearly resolved in the $0kl$ map, but it does not appear in the $hk0$ map because it is superposed on the site of the overlapping lead and vanadium atoms, and could only be brought up by an appropriate correction applied to the scaling factor for this zone. The location of O_5 in the $h0l$ map might be considered as uncertain because, from Fig. 1 alone, it might overlap either O_1 or O_2 . All doubt was removed, however, by a complete difference synthesis from which only O_5 was omitted; a small residual positive peak appeared at the O_1, O_5 position shown in the $h0l$ map of Fig. 1, whereas the electron density was virtually zero at the site of O_2 . This synthesis also indicated that O_1 and O_5 are not exactly superposed in the $0kl$ projection. The partial overlap of O_5 and O_1 also was to be expected by comparison with the corresponding $h0l$ partial difference maps for conichalcite (Qurashi & Barnes, 1963, Fig. 1) and pyrobelonite (Donaldson & Barnes, 1955, Fig. 1C). The limits of variation of the co-ordinates deduced for the oxygen atoms from pairs of maps in Fig. 1 were of the order of $\pm 0.05 \text{\AA}$. Finally, it should be observed that appreciable thermal anisotropy for Pb, and some for O_2 , is indicated in the $0kl$ and $hk0$ maps of Fig. 1.

With the co-ordinates of the metal atoms derived from the Fourier syntheses, and those of the oxygen atoms obtained from the partial

difference maps, two cycles of complete (F_o-F_c)-syntheses were carried out. The co-ordinates obtained as a result of this final refinement in $Pnma$ were Pb at 0.1287, $\frac{1}{4}$, 0.1760, Zn at 0, 0, $\frac{1}{2}$, V at 0.3690, $\frac{3}{4}$, 0.3180, O₁ at 0.189, $\frac{3}{4}$, 0.424, O₂ at 0.542, $\frac{3}{4}$, 0.415, O₃ (O₄) at 0.380, 0.984, 0.196, and O₅ at 0.152, $\frac{1}{4}$, 0.439. The R -factors at this stage were 0.04₂, 0.09₂, and 0.10₃ for the observed $hk0$, $0kl$, and $h0l$ reflections, respectively. It seemed appropriate, therefore, next to introduce the small shifts necessary to account for the weak reflections forbidden in $Pnma$.

THE NON- $Pnma$ REFLECTIONS AND THE ANTISYMMETRICAL PATTERSON AND FOURIER MAPS

The estimated values of $|F_o|$ for the four non- $Pnma$ $0kl$ reflections, recorded on a 200-hour Weissenberg film, are 17 for 025, 13 for 032, 16 for 034, and 10 for 043. None of the $hk0$ reflections forbidden in $Pnma$, however, were observed even after very long exposures, indicating, as in conicalcrite (Qurashi & Barnes, 1963), that the effects of the atomic displacements from the special positions of $Pnma$ must tend to cancel one another in this zone.

A map of the antisymmetrical Patterson (ΔP) function (Qurashi,

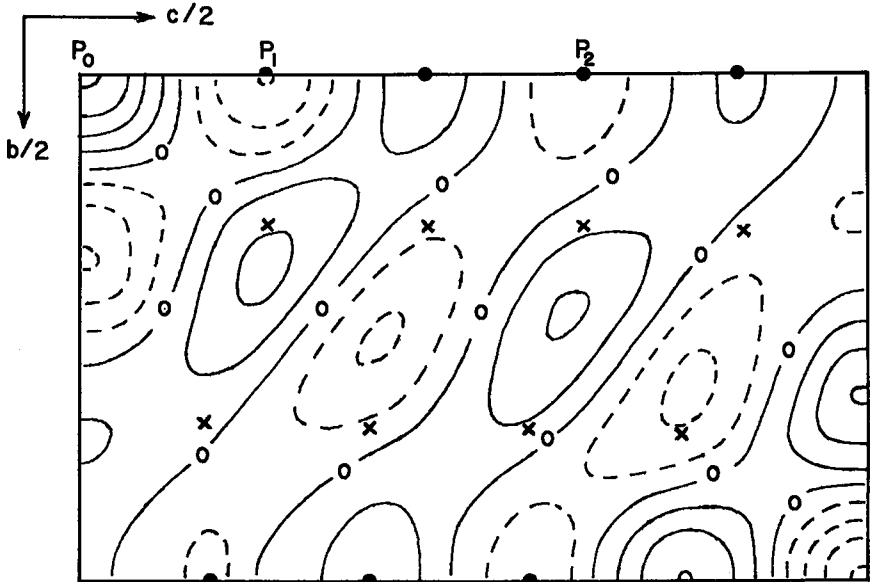


FIG. 2. Antisymmetrical Patterson $0kl$ ΔP -map. Contours at intervals of 0.1 unit with zero contours indicated by O's and negative contours by broken lines. The small solid circles mark the positive and negative non-origin peaks and the crosses show the corresponding negative and positive regions.

1963) calculated with the four $0kl$ reflections is shown in Fig. 2. The corresponding ΔP map for conichalcite (Qurashi & Barnes, 1963, Fig. 2) was taken as the starting point of the analysis, especially because the 032 and 034 reflections were among those observed in both cases. Since the height of the positive origin peak, P_o , in the $0kl$ ΔP map for descloizite is only about $1/5$ that of the origin peak in the corresponding map of conichalcite, it was to be expected that values of $Z\Delta$ for the antisymmetrical displacements (Δ) of the atoms would be lower by a factor of $(1/\sqrt{5}) = 0.45$. Furthermore, in Fig. 2, while the negative peaks at P_1 and P_2 correspond roughly to those in the conichalcite map, P_1 in descloizite is shifted towards the origin and is relatively larger compared with P_o ($P_1 \approx \frac{3}{4}P_o$). The most significant change in the map, however, is the peak at $(-\frac{1}{2}, 0)$ which is almost equal to the origin peak in the conichalcite map but is nearly zero in the descloizite map, thus indicating that the interactions between atoms with almost the same z co-ordinate, but differing by $\frac{1}{2}$ in y , are mutually opposed in descloizite instead of being superposed. From Fig. 1 it is clear that these interactions are Pb-V, $O_5-(O_2 + O_1)$ and Zn-Zn in descloizite, of which the corresponding Cu-Cu interaction in conichalcite was found to be negligible.

Other significant peaks in the ΔP map are a small negative one at $(-\frac{1}{2}, 0.08)$, and a positive one at $(-, 0, 0.22)$. From Fig. 1, the first is a possible composite of (1) Pb- O_2 , (2) O_5-O_5' (small positive, with O_5 and O_5' displacements in the same direction) and O_4-O_3' (small negative, with O_4 and O_3' displacements in opposite directions), and (3) approximately one-half the contributions of V-Pb and V- O_5 (both of which are appreciably off the peak position), (see Fig. 3(b) later). Because the net contribution from (2) is nearly zero, and that from (3) is small, while the observed negative peak is a little greater than $\frac{1}{4}P_o$, it follows that the major interaction must be Pb- O_2 and that it must be negative, and, therefore, that the Pb and O_2 shifts must be in opposite directions. It may be noted that the corresponding atoms, Ca and O_2 , in conichalcite also showed the largest displacements in that structure, and that their shifts also were in opposite directions. The small positive peak at $(-, 0, 0.22)$ arises from the overlap of so many vectors that an attempt at its full interpretation was not profitable. Finally, it was recognized that if the Zn displacements parallel to y in descloizite proved to be significant, then the Zn-Zn interactions would make a positive contribution, so that the Pb-V contribution would be negative, and the Pb and V displacements must be in opposite directions (compare the argument regarding Cu in the conichalcite structure, Qurashi & Barnes, 1963).

With a factor of 0.45 between the major shifts in descloizite compared with those in conichalcite, $(Z\Delta)_{Pb} \approx 2(Z\Delta)_V \approx 2(Z\Delta)$ for $O_2 = 0.45 \times$

$Z_m \Delta_m$ (for conichalcite) = $0.45 \times 2.4 = 1.08$. On this basis, $\Delta(\text{Pb})$, $\Delta(\text{V})$, and $\Delta(\text{O}_2)$ were evaluated and applied to the $Pnma$ y co-ordinates in order to calculate structure factors for the four observed $0kl$ reflections forbidden in $Pnma$. The results are shown in Table 1 where it is apparent that, even with Zn–Zn displacements included and based on $(Z\Delta)_{\text{Zn}} \approx \frac{1}{2} \times 1.08$, the signs for the 025, 032, and 043 reflections are definitely fixed by the contributions of Pb and O_2 alone. The sign of 034, however, is still indeterminate, probably because of the neglect of possible antisymmetrical shifts of O_5 and the O_3, O_4 pair.

Two antisymmetrical $0kl$ Fourier syntheses, therefore, were computed with $|F_c(034)|$ given a negative and a positive sign, respectively. The two maps are presented in Fig. 3(a), of which that on the right (with $F_c(034)$ positive) shows (1) a large negative peak (marked x) which is difficult to associate with any atom in the structure, (2) a relatively small displacement for Pb and an excessively large one for O_2 which is not supported by a splitting of the O_2 peak in the $hk0$ and $0kl$ partial difference maps (Fig. 1), and (3) no shifts for the O_3, O_4 pair. On the other hand, the antisymmetrical Fourier map on the left in Fig. 3(a), calculated with $F(034)$ negative, yields reasonable types of shifts for all the atoms, as indicated schematically in Fig. 3(b), with those of Pb, Zn, and O_2 as the most significant. It may be mentioned that the peak for the shift of O_3, O_4 along z is doubled relative to the others because of mutual overlap. Indirect confirmation is obtained from an examination of the last $0kl$ difference map calculated after isotropic refinement in $Pnma$ and shown on the left-hand side of Fig. 3(c), where it is apparent that appreciable anisotropy is indicated, parallel to y for Pb, Zn, and $\text{O}_2 + \text{O}_1$ (not resolved in this projection), but nearly parallel to z for the O_3, O_4 pair. In $P2_12_12_1$ such apparent anisotropy would lead to small shifts ($\sim 0.04 \text{ \AA}$) for the metal atoms and $\sim 0.2 \text{ \AA}$ for the oxygen atoms) in these directions in general agreement with the analysis of the ΔP and antisymmetrical Fourier maps. The magnitudes of the shifts estimated from Fig. 3(a), *left*, are: Pb, 0.014 \AA ; Zn, 0.020 \AA ; V = 0.010 \AA ; $\text{O}_2 + \text{O}_1$, 0.06 \AA ; O_5 , 0.04 \AA ; O_3, O_4 pair, 0.05 \AA . Because the antisymmetrical maps give the resultant shift of O_1 and O_2 ($\sim 0.06 \text{ \AA}$) while the $0kl$ and $hk0$ difference syntheses indicate an anisotropy corresponding to shifts of about 0.15 \AA for O_1 and O_2 individually, the displacement of O_1 must be in the opposite direction to that of O_2 , with $\Delta(\text{O}_2) \approx 0.2 \text{ \AA}$ and $\Delta(\text{O}_1) \approx 0.1 \text{ \AA}$. Also, there is some evidence in the $h0l$ $Pnma$ difference map (which has the same plane group symmetry in both $Pnma$ and $P2_12_12_1$), that O_3 and O_4 do not have exactly the same z co-ordinate but are displaced relative to one another, in agreement with the shifts of $\sim 0.05 \text{ \AA}$ derived from Fig. 3(a), *left*.

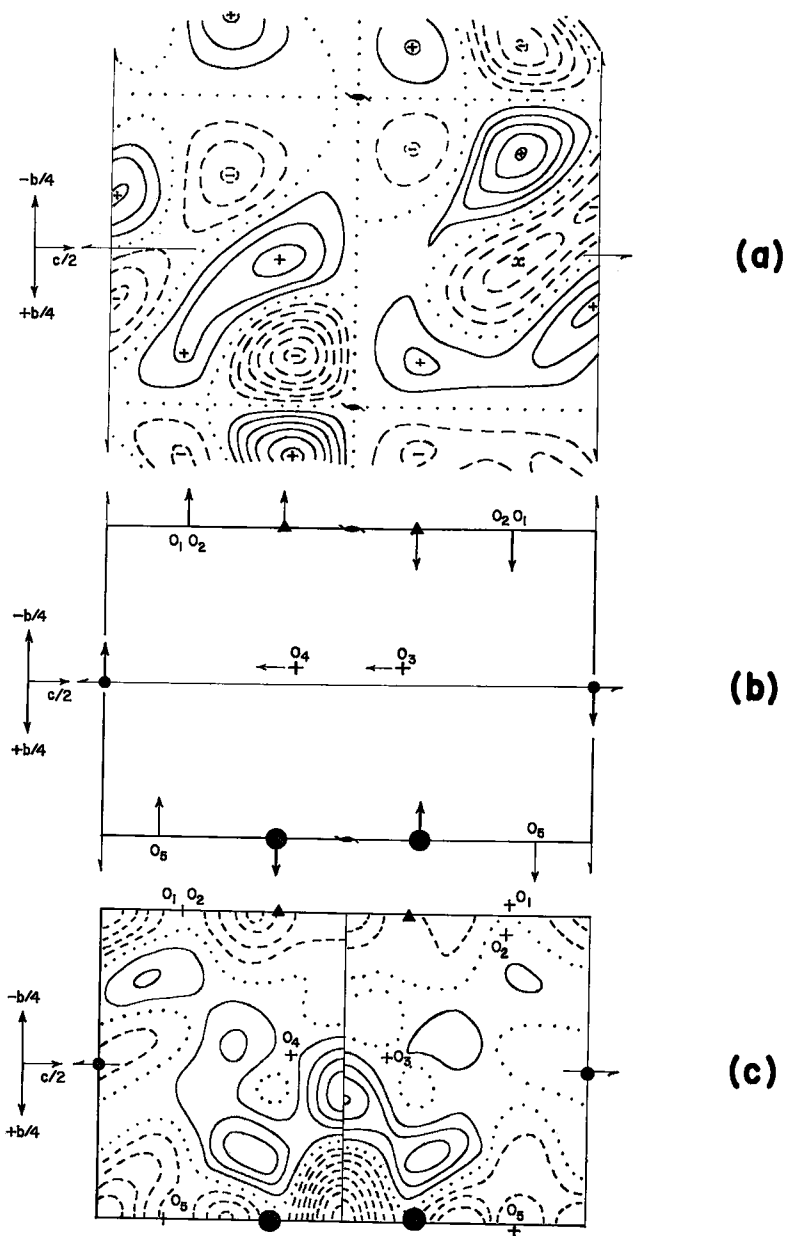


FIG. 3(a). *Left*, antisymmetrical $0kl$ Fourier synthesis with $F(034)$ negative; *right*, antisymmetrical $0kl$ Fourier synthesis with $F(034)$ positive. Contours at intervals of $0.5 e \cdot \text{\AA}^{-2}$, with zero contour dotted and negative contours broken.

(b). Directions of the antisymmetrical shifts of Pb (large solid circles), Zn (small solid circles), V (triangles) and O atoms as designated.

(c). *Left*, $(F_\sigma - F_c)$ -synthesis after isotropic refinement in $Pnma$; *right*, $(F_\sigma - F_c)$ -synthesis after final isotropic refinement in $P2_12_12_1$. Contours at intervals of $1 e \cdot \text{\AA}^{-2}$ with zero contour dotted and negative contours broken.

Values of F_c for the non- $Pnma$ reflections, calculated after application of the foregoing shifts, are shown in the last column of Table 1. The agreement with $|F_o|$ was considered to be sufficiently good ($R = 0.35$) to warrant proceeding with final refinement of the structure in $P2_12_12_1$.

TABLE 1. COMPARISON OF $|F_o|$ FOR THE NON- $Pnma$ REFLECTIONS WITH STRUCTURE FACTORS CALCULATED FOR ANTISYMMETRICAL DISPLACEMENTS OF VARIOUS GROUPS OF ATOMS

$0kl$	$F_c(\text{Pb} + \text{O}_2)$	$ F_o $	$ F_c(\text{Zn}) $	$ F_c(\text{V}) $	Sign of F	F_c
025	+12	17	4	5	+	+10
032	-14	13	0	4	-	-16
034	-5	16	0	4	?	-10
043	+12	10	5	5	+	+13

FINAL REFINEMENT IN $P2_12_12_1$

Final refinement in $P2_12_12_1$ was carried out by difference syntheses, first in the $\{0kl\}$ zone and then in the $\{hk0\}$ zone, with co-ordinates modified by the atomic shifts deduced from the antisymmetrical maps. Because of the small magnitudes of the shifts from $Pnma$ positions compared with those found in conicalcrite, improvements of the R -factors were expected to be small, and, in fact, were only 0.01 for the $0kl$ reflections and 0.002 for the $hk0$ reflections. However, the last $0kl$ difference map, calculated with isotropic temperature factors, and reproduced on the right-hand side of Fig. 3(c), shows that the anisotropies evident in the corresponding map after isotropic refinement in $Pnma$ (Fig. 3(c), left) have been reduced by about one-third to two-thirds. Furthermore, all values of F_c for the unobserved $0kl$ and $hk0$ reflections are < 15 (mean, 5.3) which compares favourably with the estimated threshold values of 12 and 14 for the two zones.

The final refinement cycle, with the inclusion of anisotropic temperature factors for Pb, Zn and V reduced R to 0.04₀, 0.07₂, and 0.10₁ for the $hk0$, $0kl$, and $h0l$ reflections, respectively, based on the observed data only, and to 0.06₀, 0.09₄, and 0.11₂, respectively, when the unobserved reflections, with $|F_o|$'s taken as one-half of the threshold values, were included.

The final values of the fractional co-ordinates, referred to the $Pnma$ origin, are listed in Table 2, separately for the three principal zones, together with their mean values. The root-mean-squares (r.m.s.) of one-half the differences between the two values of each co-ordinate for the five oxygen atoms collectively are $0.002a = 0.015 \text{ \AA}$, $0.0068b = 0.041 \text{ \AA}$, and $0.006c = 0.043 \text{ \AA}$. The r.m.s. deviations for the three co-ordinates

(converted to Å) for each oxygen atom separately are 0.037 Å for O₁, 0.041 Å for O₂, 0.008 Å for O₃, 0.012 Å for O₄, and 0.055 Å for O₅ (OH), with a mean of 0.031 Å. The corresponding r.m.s. values for the lead and vanadium atoms are 0.003₆ Å and 0.006 Å, respectively. The displacement of the zinc atoms from the special position 0, 0, $\frac{1}{2}$ is only 0.0032*b* = 0.02 Å, with a probable uncertainty of about 0.004 Å. The estimated standard deviations, calculated according to the formula of Cruickshank (1949), are 0.002 Å for Pb, 0.006 Å for Zn, 0.008 Å for V, and 0.038 Å for the five O. The means of both estimations are 0.003 Å for Pb, 0.005 Å for Zn, 0.007 Å for V, and 0.034 Å for O, from which the e.s.d.'s of the metal-

TABLE 3. STRUCTURE FACTOR DATA SEPARATELY FOR THE THREE PRINCIPAL ZONES (P₂1₂1₁)

<i>Ok</i> l	F _o	F _c	<i>Ok</i> l	F _o	F _c	<i>Ok</i> l	F _o	F _c
002	128	+125.6	025	17	+8.6	045	<12	+4.8
004	29	-1.3	026	114	-118.1	046	181	-201.7
006	277	-281.3	027	<12	-6.8	047	<12	+1.3
008	156	-160.2	028	234	-220.6	048	118	-112.7
0.0.10	76	-76.8	029	<12	-2.4	051	88	-88.3
011	172	-173.7	0.2.10	<12	+22.9	052	<12	-10.8
012	<12	-1.7	031	140	-148.6	053	16	-7.2
013	45	-41.6	032	13	-13.9	054	<12	-14.6
014	<12	-3.5	033	31	-32.7	055	47	+72.0
015	150	+136.2	034	16	-15.1	056	<12	-3.3
016	<12	-2.5	035	116	+109.5	057	84	+85.9
017	146	+152.2	036	<12	-1.9	060	123	+110.8
018	<12	-2.5	037	134	+125.3	061	<12	+7.0
019	29	+31.5	038	<12	+6.6	062	116	+117.5
0.1.10	<12	-1.6	039	35	+33.1	063	<12	+2.4
0.1.11	47	-56.4	040	355	+364.6	064	81	-78.5
020	239	+270.0	041	<12	-6.1	065	<12	+11.2
021	<12	+2.4	042	82	+79.4	066	66	-69.4
022	205	+220.6	043	10	+16.4	071	72	-61.2
023	<12	+1.6	044	<12	+3.1	072	<12	-11.1
024	186	-178.2						

<i>hk</i> 0	F _o	F _c	<i>hk</i> 0	F _o	F _c	<i>hk</i> 0	F _o	F _c
020	239	-273.2	270	111	-109.8	530	<14	-5.4
040	355	+370.9	310	<14	+4.5	540	<14	-5.4
060	123	-120.4	320	<14	-10.9	550	<14	+6.4
110	<14	-6.2	330	<14	-9.1	600	89	-102.3
120	<14	-0.4	340	<14	+8.0	610	237	-225.7
130	<14	+13.0	350	<14	+10.5	620	<14	-4.0
140	<14	+10.8	360	<14	-14.4	630	173	+183.0
150	<14	-13.3	370	<14	-8.5	640	75	-72.5
160	<14	-2.1	400	250	-236.6	650	144	-141.8
170	<14	+11.0	410	34	+37.9	710	<14	-0.9
200	75	-79.3	420	298	+297.5	720	<14	+2.9
210	347	+352.2	430	32	-31.2	730	<14	+1.9
220	117	-113.5	440	154	-153.4	800	184	+186.9
230	265	-261.3	450	15	+20.1	810	28	-36.4
240	51	-49.1	460	142	+154.4	820	82	-79.1
250	190	+192.0	510	<14	+1.8	830	33	+32.8
260	56	-52.0	520	<14	+7.6			

TABLE 3.—concluded.

hOl	$ F_o $	F_o	hOl	$ F_o $	F_o	hOl	$ F_o $	F_o
002	128	-122.5	209	27	+24.3	504	131	-113.6
004	29	+17.4	2.0.10	24	+22.1	505	132	-117.9
006	277	+265.8	301	155	-138.5	506	<25	+27.9
008	156	-159.4	302	142	-131.6	507	35	-52.3
0.0.10	76	+69.7	303	127	+129.2	508	41	+35.7
101	<25	-6.1	304	108	+110.6	509	32	+41.2
102	107	-117.4	305	214	-210.6	600	89	+101.0
103	315	-302.6	306	25	-27.6	601	74	+76.7
104	165	+175.5	307	66	-69.3	602	28	+41.7
105	34	+43.1	308	28	-28.9	603	<25	-15.3
106	26	-32.5	309	35	+49.5	604	28	+50.4
107	26	-38.6	3.0.10	51	+58.1	605	84	-78.1
108	46	-41.0	400	250	-242.0	606	36	+51.7
109	158	-125.8	401	<25	+13.1	607	96	+71.6
1.0.10	59	+54.3	402	282	+264.0	701	<25	+4.9
1.0.11	56	+62.6	403	<25	-2.5	702	54	+59.6
200	75	+80.8	404	111	+103.6	703	170	-173.7
201	162	-155.8	405	<25	+3.3	704	56	-56.5
202	108	+102.7	406	161	-136.2	705	47	+52.6
203	44	-45.2	407	<25	+5.9	706	21	+17.5
204	59	+75.5	408	204	+188.0	707	42	-30.9
205	82	+89.0	409	<25	-11.7	800	184	+191.8
206	39	+50.4	501	138	-135.1	801	<25	-12.7
207	131	-113.8	502	58	+72.5	802	54	-59.7
208	37	+54.5	503	52	+59.7	803	<25	-2.6

oxygen distances are 0.034 Å for Pb-O and for Zn-O, and 0.035 Å for V-O.

The calculated structure factors are compared with the observed structure amplitudes separately for each zone in Table 3. The co-ordinates employed were those given in Table 2 but referred to the standard origins of the principal projections (pgg) of $P2_12_12_1$. The atomic scattering factors for V^{+2} and O^{-1} given by Freeman (1959) were employed, while those for Zn^{+2} were obtained by interpolation between the values of Cu^{+2} and Ga^{+2} tabulated by Watson & Freeman (1961), and those for Pb^{+2} were based on the values for Tl^{+2} of Freeman (1959). The final anisotropic temperature-factor constants for Pb, Zn, and V in each zone are shown in Table 4; an isotropic value of $B = 1.3 \text{ \AA}^2$ was employed for each oxygen atom in all three zones. In the case of Pb an analysis of the anisotropic temperature-factor constants leads to $B_x = 1.7_6 \pm 0.02 \text{ \AA}^2$, $B_y = 1.8_4 \pm 0.06 \text{ \AA}^2$, and

TABLE 4. TEMPERATURE-FACTOR CONSTANTS (B) FOR THE METAL ATOMS SEPARATELY IN THE THREE PRINCIPAL ZONES

Atom	$\{0kl\}$	$\{hOl\}$	$\{hk0\}$
Pb	1.45 ± 0.45	1.75 ± 0.30	1.78
Zn	1.1 ± 0.2	1.5 ± 0.5	1.2
V	0.8	0.4	1.0

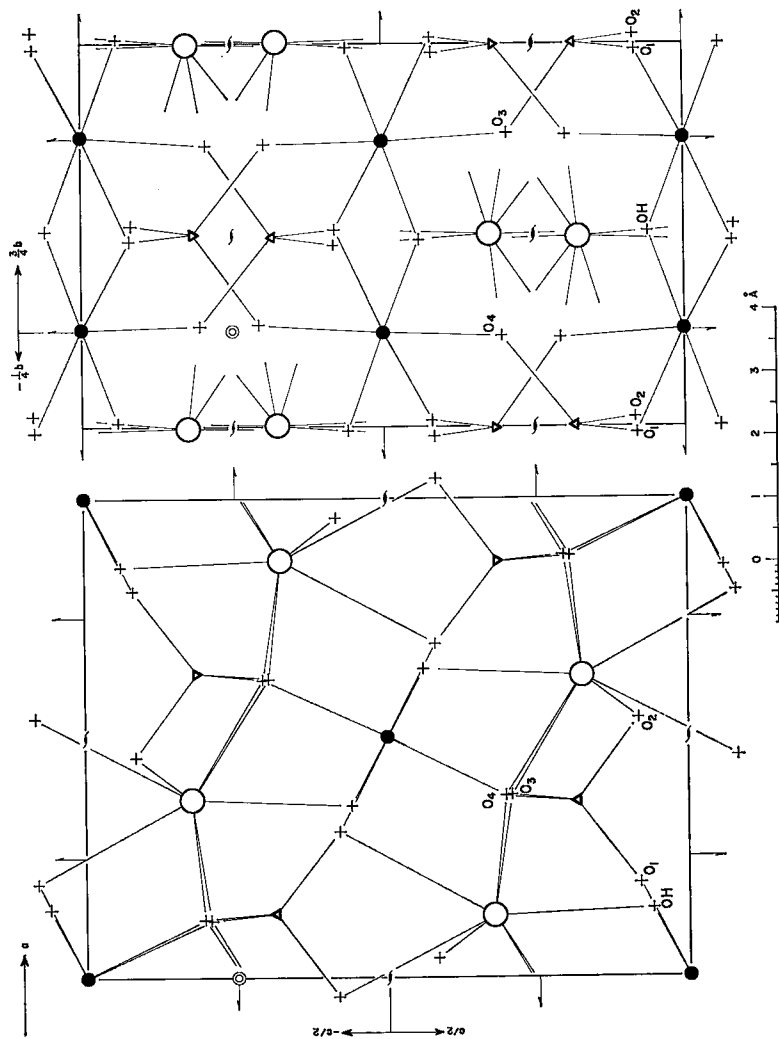


FIG. 4. Projections of descloizite along $[010]$ and $[100]$; $Pnma$ origin. The $P2_12_12_1$ origin is indicated in each projection by a double circle. Large open circles, Pb; small solid circles, Zn; triangles, V; crosses, O. To avoid confusion, two Zn-O bonds (of an overlapping bipyramid) have been omitted from the centre of the $[010]$ projection, and only the directions of the Zn-O bonds have been indicated (by short lines) in the $[100]$ projection.

$B_z = 1.37 \pm 0.37 \text{ \AA}^2$. For Zn the greatest thermal motion appears to be in the yz plane ($B_{yz} \sim 1.4 \text{ \AA}^2$).

The mean co-ordinates of Table 2, but referred to the $P2_12_12_1$ origin (halfway between the three pairs of non-intersecting screw axes) are given in Table 5. There were no outstanding features in the final difference maps, where the residual electron densities varied between $\pm 2.2 e.\text{\AA}^{-2}$ and $\pm 5 e.\text{\AA}^{-2}$. Projections of the structure along $[010]$ and $[100]$ are presented in Fig. 4, where only the oxygen atoms with the specific co-ordinates shown in Table 5 (together with O_1 and O_2 at $x, 1+y, z$) are labelled.

TABLE 5. FRACTIONAL ATOMIC CO-ORDINATES:
 $P2_12_12_1$ ORIGIN

Atom	x	y	z
Pb	0.128 ₇	0.253 ₄	0.426 ₀
Zn	0.0000	0.003 ₂	0.7500
V	0.367 ₀	-0.246 ₀	0.565 ₀
O_1	0.196	-0.265	0.670
O_2	0.540	-0.226	0.668
O_3	0.380	0.516	0.456
O_4	0.379	-0.013	0.447
O_5 (OH)	0.142	0.260	0.691

DISCUSSION

The structure of descloizite is very similar to that of the isomorphous arsenate, conicalcite ($\text{CaCu}(\text{AsO}_4)(\text{OH})$), (Qurashi & Barnes, 1963). All V to O distances $< 3.4 \text{ \AA}$, all Zn to O distances $< 3.6 \text{ \AA}$, and all Pb to O distances $< 3.4 \text{ \AA}$, are collected in Table 6, together with the O-O distances which constitute edges of the oxygen co-ordination polyhedra around V, Zn, and Pb.

There is a slightly distorted tetrahedral co-ordination of oxygen atoms around V, with the edges given in Table 6 and O-V-O angles of 106° (three), 110° , 111° , and 118° (mean, 109.5°). The oxygen atoms around Zn are at the corners of a distorted tetragonal bipyramid with O_1 , O_5 (OH), O_1' , O_5' (OH') defining the equatorial plane, and with O_3 and O_4 at the apices.

There is 8-fold co-ordination, in the form of distorted square antiprisms, around the lead atoms, with the "square" faces represented by O_1 , O_2' , O_3 , O_4' and O_2 , O_4 , O_5 (OH), O_3 . In a structure recently reported by Bachmann & Zemmann (1961) for linarite, $\text{PbCu}(\text{SO}_4)(\text{OH})_2$, there are three short Pb-O distances (2.38 \AA , 2.44 \AA (two)), and five longer ones (2.82 \AA , 2.97 \AA , 3.00 \AA , 3.06 \AA (two)), which are comparable with those in descloizite, but the spatial arrangement of these eight oxygen atoms

bears no resemblance to a square antiprism. No special significance can be attached to this difference, however, because of the relatively small number of complex structures involving lead and oxygen which have been examined to date. In brackebuschite, $\text{Pb}_2(\text{Mn,Fe})(\text{VO}_4)_2 \cdot \text{H}_2\text{O}$ for example, two crystallographically non-equivalent lead atoms have eight and ten nearest oxygen neighbours with Pb–O distances of 2.54 to 2.95 Å, and 2.58 to 3.02 Å, respectively (Donaldson & Barnes, 1955*b*). The polyhedron defined by the former, however, does not take the form of a square antiprism.

In pyrobelonite, $\text{PbMn}(\text{VO}_4)(\text{OH})$, the co-ordination around Pb has been reported as 7-fold (Pb–O = 2.28 to 2.89 Å) with two other oxygen atoms at distances of 3.28 Å each from Pb (Donaldson & Barnes, 1955*a*). At the time of this structure investigation, no excessively long exposure times were employed for precession or Weissenberg photographs and no reflections forbidden by *Pnma* were observed. In view of the current refinements of the structures of conichalcite and descloizite, however, it became of interest to see if any weak reflections could be detected which would reduce the space group of pyrobelonite to $P2_12_12_1$. Accordingly, an *0kl* Weissenberg photograph of pyrobelonite was given 180 hours of exposure, and two weak spots corresponding to the 025 and 032 reflections appeared on each of two films. Both of these non-*Pnma* reflections were observed from descloizite and the second also from conichalcite. The true space group of pyrobelonite, therefore, is $P2_12_12_1$ which is the same as that of conichalcite, descloizite, and adelite, $\text{CaMg}(\text{AsO}_4)(\text{OH},\text{F})$ (Hägele, 1939). Comparison of the *Pnma 0kl* difference map for descloizite, reproduced in the present Fig. 3(a) *left*, with the corresponding left half of Fig. 2D for pyrobelonite (Donaldson & Barnes, 1955*a*, p. 587) shows similar indications of some apparent anisotropy particularly at the sites of O_1 , O_2 , O_3 (O_4), O_5 and Pb. At least a part of these effects has been found to arise in descloizite from the fact that the true locations of these atoms are displaced from *Pnma* positions. It seems clear, therefore, that similar small shifts must occur also in pyrobelonite. One of the effects of a displacement of O_2 would be to increase the length of one of the long (3.28 Å) Pb–O distances and decrease the length of the other. This would complete an 8-fold distorted square antiprismatic co-ordination polyhedron of oxygen atoms around Pb and would probably also increase the length of the very short (2.28 Å) bond to OH.

The co-ordination polyhedra around V, Zn, and Pb in descloizite, together with their shared edges and corners, are the same (with the exception of the numerical values of specific interatomic distances and angles) as those around As, Cu, and Ca, respectively, in conichalcite, so that it is unnecessary to repeat the detailed description given in the

discussion of the conichalcite structure (Qurashi & Barnes, 1963). For purposes of comparison, in addition to the data shown in Table 6, the metal-metal separations across the shared edges in descloizite are V-Pb, 3.41 Å and 3.60 Å; Pb-Pb, 4.05 Å (two); Pb-Zn, 3.55 Å and 3.56 Å (across O-OH), and 3.60 Å and 3.63 Å (across O-O); Zn-Zn, 3.04 Å (two, across O-OH).

It may also be noted that, in descloizite as in conichalcite, the only two oxygen atoms not co-ordinated with the same cation are O_5 and O_2 . The atom O_5 has been identified with the OH group in conichalcite (Qurashi & Barnes, 1963), and the O_5 (OH) distance in descloizite is only 2.76 Å, O_2 being closer to OH than any other oxygen atom. The angles Pb-OH- O_2 = 121°, Zn-OH- O_2 = 109°, and Zn'-OH- O_2 = 112° (mean, 114°). It is possible, therefore, that a H-bond exists between OH and O_2 .

The lengths of the tetrahedral V- O_1 and V- O_2 bonds (each, 1.64 Å), and the V- O_3 (1.78 Å) and V- O_4 (1.80 Å) bonds suggest that the two latter represent essentially single bonds, while the first two possess a large proportion of double bond character (see Bachmann & Barnes, 1961, p. 227). The lengths of the tetrahedral V-O bonds in pyrobelonite are 1.62 Å, 1.77 Å (two) and 1.83 Å (Donaldson & Barnes, 1955*a*), although the suspected shifts required of some of the atoms in this structure would result in some alterations to these values; they are 1.72 Å (two), 1.83 Å, and 1.86 Å in brackebuschite (Donaldson & Barnes, 1955*b*), and 1.72 Å (two) and 1.76 Å (two) in vanadinite (Trotter & Barnes, 1958). The variations in the bond lengths within the VO_4 tetrahedron from one structure to another probably arises from the varying effects of the different cations. In pucherite, $BiVO_4$, there are two long V-O bonds of 1.95 Å each in addition to two of 1.76 Å (Qurashi & Barnes, 1953). Although the two of 1.95 Å are no longer than some of the medium bonds in the trigonal bipyramidal co-ordination around V which is characteristic of the meta-vanadates, rossite (Ahmed & Barnes, 1963) and metarossite (Kelsey & Barnes, 1960), they are appreciably longer than now would be expected for tetrahedral co-ordination around pentavalent vanadium. It is possible, therefore, as suggested previously (Qurashi & Barnes, 1953, p. 499), that the vanadium in pucherite has a lower valence number than +5.

ACKNOWLEDGMENTS

Grateful acknowledgment is made to Dr. F. R. Ahmed and to Mrs. M. E. Pippy of this laboratory for carrying out most of the structure factor, electron density, and bond length calculations on IBM 650 and 1620 computers with programmes written by Dr. F. R. Ahmed.

REFERENCES

- AHMED, F. R. & BARNES, W. H. (1963): The crystal structure of rossite, *Can. Mineral.*, **7**, 713-726.
- BACHMANN, H. G. & BARNES, W. H. (1961): Bonding in the trigonal bipyramidal coordination polyhedra of V_2O_5 and of certain other structures containing pentavalent vanadium, *Zeit. Krist.*, **115**, 215-230.
- BACHMANN, H. G. & ZEMANN, J. (1961): Die Kristallstruktur von Linarit, $PbCuSO_4(OH)_2$, *Acta Cryst.*, **14**, 747-753.
- BARNES, W. H. & QURASHI, M. M. (1952): Unit cell and space group data for certain vanadium minerals, *Am. Mineral.*, **37**, 407-422.
- CRUICKSHANK, D. W. J. (1949): The accuracy of electron-density maps in x -ray analysis with special reference to dibenzyl, *Acta Cryst.*, **2**, 65-82.
- DONALDSON, D. M. & BARNES, W. H. (1955a): The structures of the minerals of the descloizite and adelite groups: II—pyrobelonite, *Am. Mineral.*, **40**, 580-596.
- (1955b): The structures of the minerals of the descloizite and adelite groups: III—brackebuschite, *ibid.*, 597-613.
- FREEMAN, A. J. (1959): Atomic scattering factors for spherical and aspherical charge distributions, *Acta Cryst.*, **12**, 261-271.
- HÄGELE, G. (1939): Adelit und Descloizit, *N. Jahrb. Min. Abt. A, Beil.-Bd.* **75**, 101-109. *Internationale Tabellen zur Bestimmung von Kristallstrukturen* (1935), Borntraeger, Berlin.
- KELSEY, C. H. & BARNES, W. H. (1960): The crystal structure of metarossite, *Can. Mineral.*, **6**, 448-466.
- QURASHI, M. M. (1954): On the completion and extension of the table of atomic scattering factors published by Viervoll and Ögrim, *Acta Cryst.*, **7**, 310-312.
- (1963): Use of the anti-symmetric component of the Patterson and Fourier functions for the solution of problems involving small atomic shifts from positions of super-symmetry, *Acta Cryst.*, **16**, 307-310.
- QURASHI, M. M. & BARNES, W. H. (1953): The structure of pucherite, $BiVO_4$, *Am. Mineral.*, **38**, 489-500.
- (1954): The structures of the minerals of the descloizite and adelite groups: I—descloizite and conicalcite (part 1), *loc. cit.*, **39**, 416-435.
- (1963): The structures of the minerals of the descloizite and adelite groups: IV—descloizite and conicalcite (part 2), the structure of conicalcite, *Can. Mineral.*, **7**, 561-577.
- QURASHI, M. M., BARNES, W. H. & BERRY, L. G. (1953): The space group of conicalcite, *Am. Mineral.*, **38**, 557-559.
- TROTTER, J. & BARNES, W. H. (1958): The structure of vanadinite, *Can. Mineral.*, **6**, 161-173.
- VIERVOLL, H. & ÖGRIM, O. (1949): An extended table of atomic scattering factors, *Acta Cryst.*, **2**, 277-279.
- WATSON, R. E. & FREEMAN, A. J. (1961): Hartree-Fock atomic scattering factors for the iron transition series, *Acta Cryst.*, **14**, 27-37.

Manuscript received September 4, 1962.